

## MASS CONSTRAINTS FROM ECLIPSE TIMING IN DOUBLE WHITE DWARF BINARIES

DAVID L. KAPLAN<sup>1</sup>KITP, Kohn Hall, University of California, Santa Barbara, CA 93106, USA; dkaplan@kitp.ucsb.edu  
*ApJ*, in press

## ABSTRACT

I demonstrate that an effect similar to the Römer delay, familiar from timing radio pulsars, should be detectable in the first eclipsing double white dwarf (WD) binary, NLTT 11748. By measuring the difference of the time between the secondary and primary eclipses from one-half period (4.6 s), one can determine the physical size of the orbit and hence constrain the masses of the individual WDs. A measurement with uncertainty  $< 0.1$  s—possible with modern large telescopes—will determine the individual masses to  $\pm 0.02 M_{\odot}$  when combined with good-quality ( $< 1 \text{ km s}^{-1}$ ) radial velocity data, although the eccentricity must also be known to high accuracy ( $\pm 10^{-3}$ ). Mass constraints improve as  $P^{-1/2}$  (where  $P$  is the orbital period), so this works best in wide binaries and should be detectable even for non-degenerate stars, but such constraints require the mass ratio to differ from one and undistorted orbits.

*Subject headings:* binaries: eclipsing—stars: individual (NLTT 11748)—techniques: photometric—white dwarfs

## 1. INTRODUCTION

Since the discovery of binary pulsars (Hulse & Taylor 1975), precision timing (typical uncertainties  $< 1 \mu\text{s}$ ) has been used to derive a variety of physical constraints (see the discussion in Lorimer & Kramer 2004). The arrival-time delay across the orbit (the Römer delay<sup>2</sup>) immediately gives the projected semimajor axis of the pulsar (Blandford & Teukolsky 1976). This, especially when coupled with the relatively narrow mass distribution of neutron stars (Thorsett & Chakrabarty 1999), constrains the mass of the companion.

I contrast this with eclipse timing of planetary systems (typically uncertainties are  $\gtrsim$  seconds). Here, with a mass ratio  $\approx 10^{-3}$  the radial velocity curve gives a limit on the mass of the companion planet. With transiting systems,  $\sin i \approx 1$  and the mass of the planet is further constrained but not known uniquely (Charbonneau et al. 2000), although with knowledge of the stellar parameters one can infer the planetary mass and radius (e.g., Brown et al. 2001). If individual eclipses can be timed to high precision (and here I mean both primary and secondary eclipses, i.e., transits and occultations), one can learn more about the system (e.g., Winn 2010). Variations in the eclipse times can unveil the presence of additional bodies in the system (e.g., Agol et al. 2005; Holman & Murray 2005), precession (e.g., Miralda-Escudé 2002), and kinematics of the system (Rafikov 2009).

With the recent discovery (Steinfadt et al. 2010b) of NLTT 11748, an eclipsing double white dwarf (WD) binary with a tight enough orbit that the binary will merge within a Hubble time, a whole new series of questions may be asked. The initial constraints are the radial velocity amplitude of the lighter object (owing to the inverted mass–radius relation of WDs, this object

is the larger and brighter member of the system) and the widths and depths of both transit and occultation. From this, assuming a cold C/O WD for the heavier object, Steinfadt et al. (2010b) were able to limit the masses and radii of both objects, but could not determine unique constraints. Measurement of spectral lines from the fainter object would determine both masses uniquely, but this is challenging as the fainter object is only  $\approx 3.5\%$  of the flux of the brighter.

A number of other close WD binaries have been discovered in the last 2 years (see Table 1 for those with undetermined inclinations). Most of them, like NLTT 11748, appear to have a low-mass ( $\lesssim 0.2 M_{\odot}$ ) He WD in orbit with a more massive ( $0.5\text{--}1.0 M_{\odot}$ ) C/O WD. Such systems are of interest because of their eventual evolution, with mass transfer brought on by gravitational radiation (Nelemans et al. 2001) and are presumed to be the progenitors of highly variable objects: R CrB stars, AM CVn binaries, and Type Ia supernovae (Iben & Tutukov 1984; Webbink 1984). Many of these binaries are also of immediate interest as verification targets for the *Laser Interferometer Space Antenna* (LISA) mission (Nelemans 2009).

Of the 11 compact WD binaries known, only NLTT 11748 is known to be eclipsing, but searches for the other sources are not uniformly constraining and additional systems may yet be discovered. The flux ratios vary for the systems, and in some cases it may be easier to directly measure the radial velocity curves for both members of the binary. Without two radial velocity curves, mass constraints are limited. Such constraints are invaluable in understanding the detailed formation histories and expected evolution of these systems as well as in determining the mass–radius relation from eclipse measurements. Moreover, their use as LISA verification sources is improved by accurate knowledge of the binary parameters. In this Letter, I discuss an effect that uses precision timing of the eclipses in such double WD systems to help constrain the individual masses of the WDs. This technique is known in other contexts, being common in ra-

<sup>1</sup> *Hubble* Fellow<sup>2</sup> The Römer delay is named after O. Römer, who used deviations from periodicity in the eclipses of Io by Jupiter to deduce a finite speed of light (Sterken 2005b).

TABLE 1  
DOUBLE WDs THAT WILL MERGE WITHIN A HUBBLE TIME AND MAY BE ECLIPSING

Object	$P_{\text{Orb}}$ (hr)	$K_2$ (km s $^{-1}$ )	$M_1$ ( $M_{\odot}$ )	$R_1$ ( $R_{\odot}$ )	$M_2$ ( $M_{\odot}$ )	$R_2$ ( $R_{\odot}$ )	$\Delta t_{\text{LT}}$ (s)	Refs.
SDSS J1053+5200	1.02	265	0.26	> 0.017	0.20	0.04	0.2	1,2
SDSS J1436+5010	1.10	347	0.45	0.014	0.22	0.04	0.7	1,2
SDSS J0849+0445	1.89	367	0.65	0.012	0.17	0.05	2.0	1
WD 2331+290	4.08	156	0.39	0.015	0.32	0.016	0.5	3,4,5
SDSS J1257+5428	4.55	323	0.92	0.009	0.15	0.04	4.7	6,7,8
NLTT 11748	5.64	271	0.74	0.010	0.15	0.04	4.6	9,10
SDSS J0822+2753	5.85	271	0.71	0.010	0.17	0.04	4.7	1

REFERENCES. — 1: Kilic et al. (2010); 2: Mullally et al. (2009); 3: Marsh, Dhillon, & Duck (1995); 4: Nelemans et al. (2005); 5: Liebert, Bergeron, & Holberg (2005); 6: Badenes et al. (2009); 7: Kulkarni & van Kerkwijk (2010); 8: Marsh et al. (2010); 9: Kawka & Vennes (2009); 10: Steinfadt et al. (2010b)

NOTE. — The values for  $M_1$  assume an edge on orbit, i.e.,  $\sin i = 1$ . The values for  $R_1$  were calculated from those values assuming a cold C/O WD (Althaus & Benvenuto 1998). Additional double-WD binaries exist, but they have inclinations known to exclude eclipses.

dio pulsar systems and planetary systems (Knutson et al. 2007; Hebrard et al. 2010; Agol et al. 2010), although in the latter it is largely a nuisance parameter and does not constrain the systems. I discuss its applicability to eclipsing double WD systems, the required observational precision and the resulting accuracy.

## 2. LIGHT TRAVEL DELAY AND MASS CONSTRAINTS

In a system with a circular orbit, one often speaks of the primary and secondary eclipses as occurring exactly  $1/2$  period apart, but this is not the case. If the members of the binary are of unequal mass the finite speed of light will cause an apparent shift in the phase of the secondary eclipse from  $P/2$ , where  $P$  is the period of the binary (Loeb 2005; Fabrycky 2010). This is similar to the shifts in eclipse timing caused by a perturbing third body on a binary system (Schneider & Doyle 1995; Doyle et al. 1998; Deeg et al. 2000; Sterken 2005a; Lee et al. 2009; Qian et al. 2009), although here one only requires two bodies and the frequency of the shift is known.

In the case of a planet with mass  $m \ll M$  orbiting a star with mass  $M$ , one has a primary eclipse when the planet is in front of the star. The light is blocked at time  $t = 0$ . However, that light was emitted earlier by the star, at time  $t_1 = 0 - a/c$ , since it traveled a distance  $a$  (the semimajor axis). For the secondary eclipse, the light is emitted by the planet at time  $t = P/2$  but is blocked  $a/c$  later, at  $t_2 = P/2 + a/c$ . The difference of these times exceeds  $P/2$  by  $\Delta t_{\text{LT}} = t_2 - t_1 - P/2 = 2a/c$ , the sought-after quantity.

For two finite masses, I consider two objects orbiting their center of mass with period  $P$ , masses  $M_1$  and  $M_2$ , and semimajor axis  $a$ . The total mass of the system is  $M = M_1 + M_2$ , and of course  $4\pi^2 a^3 = P^2 GM$ ; the first object orbits at a radius  $a_1 = a(M_2/M)$  and the second object orbits at a radius  $a_2 = a(M_1/M)$ .

Near primary eclipse, the primary is at  $[x, y] = [2\pi a_1 t/P, a_1]$  and the secondary is at  $[-2\pi a_2 t/P, -a_2]$  at time  $t$ , with the observer at  $[0, -\infty]$ . I project the image of the two objects to the barycenter at  $y = 0$ . This gives  $x_{\text{B},1} = 2\pi a_1(t - a_1/c)/P$  and  $x_{\text{B},2} = -2\pi a_2(t + a_2/c)/P$ . Eclipses occur when these are equal, which has the solution  $t_1 = (a_1 - a_2)/c$ . Near secondary eclipse, the

primary is at  $[-2\pi a_1(t - P/2)/P, a_1]$  and the secondary is at  $[2\pi a_2(t - P/2)/P, -a_2]$ . Following the same argument, eclipses occur when  $t_2 - P/2 = (a_2 - a_1)/c$ . So the eclipses differ by  $t_2 - t_1 = P/2 + 2(a_2 - a_1)/c$ . The light-travel delay is again  $\Delta t_{\text{LT}} = t_2 - t_1 - P/2$ ,

$$\Delta t_{\text{LT}} = \left(\frac{2}{c}\right)(a_2 - a_1) = \left(\frac{2a}{c}\right)\left(\frac{M_1 - M_2}{M_1 + M_2}\right), \quad (1)$$

reaching  $2a/c$  when  $M_2 \ll M_1$ , as expected. From Kepler's laws the mass function  $K_2^3 P/2\pi G = M_1^3 \sin^3 i M^{-2}$ , where  $K_2$  is the radial velocity amplitude of object 2, and since it is a transiting system,  $\sin i \approx 1$ . Substituting for  $a$  and the masses, the time delay in terms of observables and the mass ratio  $q$  (where  $q = M_2/M_1 \leq 1$ ) is:

$$\Delta t_{\text{LT}} = \frac{PK_2}{\pi c}(1 - q). \quad (2)$$

### 2.1. Magnitude and Detectability

The eclipse duration for a circular orbit is roughly  $T \approx 2R_2 P/(2\pi a) \approx 3$  minutes (Winn 2010); the duration of ingress/egress  $\tau$  is decreased by a factor of  $R_1/2R_2 \approx 8$ ,  $\tau \approx R_1 P/(2\pi a) \approx 20$  s (numerical results are for NLTT 11748); and ingress/egress are sharpest at inclinations of exactly  $90^\circ$ . The accuracy of the eclipse time determination largely depends on the duration of the ingress/egress and the total number of photons accumulated during ingress/egress, since the bottom of the eclipse is only slightly curved (for the primary eclipse) if not flat (secondary eclipse), and one can derive (e.g., Carter et al. 2008)

$$\sigma_{t_c} = \frac{\sigma}{\delta} \frac{\tau}{\sqrt{2N_{\text{obs}}}}, \quad (3)$$

where the eclipse has fractional depth  $\delta$ , each observation has fractional uncertainty  $\sigma$ , and there are  $N_{\text{obs}}$  observations during  $\tau$ . This holds in the limit that the noise is uncorrelated (cf. Carter & Winn 2009; Sybilski et al. 2010), which should be true at the level discussed here (photometric precision of  $\gtrsim$  mmag). So,  $\sigma_{t_c}$  scales as the

duration of ingress/egress divided by the total signal-to-noise ratio accumulated during that portion of the orbit. Since  $N_{\text{obs}} \propto \tau$  for a constant observing cadence,  $\sigma_{t_e} \propto \sqrt{\tau}$ . A star with  $V = 16.5$  mag like NLTT 11748 gives roughly  $0.1 \text{ photons s}^{-1} \text{ cm}^{-2}$  or  $2 \times 10^5$  photons detected during a 20 s ingress/egress with a 4 m telescope. For an eclipse depth of 5% this means a precision on individual eclipse times of  $< 1$  s.

For general binary systems, I can rewrite the expression for  $\Delta t_{\text{LT}}$  in terms of the primary mass  $M_1$ ,  $q$ , and  $P$  (eliminating  $K_2$ ):

$$\Delta t_{\text{LT}} = \left( \frac{2GM_1 P^2}{\pi^2 c^3} \right)^{1/3} \frac{(1-q)}{(1+q)^{2/3}} \quad (4)$$

For systems with primaries that are typical C/O WDs and with secondaries that are He WDs, with  $M_1 = 0.5 - 1 M_\odot$  and  $q = 1/6 - 1/2$ ,  $\Delta t_{\text{LT}}$  goes from 0.5 s to 7 s for periods of 0.5–10 hr (Table 1).

Eclipse depths are functions of the radii and temperatures of the WDs, as well as the bandpass, and are hard to predict with any generality. The main factor that will change systematically for other double WD systems is  $\tau$  itself, which is  $\propto R_1 P^{1/3}$ . This means the signal-to-noise ratio (i.e., detectability) is  $\Delta t_{\text{LT}}/\sigma_{t_e} \propto \sqrt{P/R_1}$ , so the effect is easiest to see in long-period binaries. As the mass ratio approaches 1 the magnitude of the delay decreases, limiting its utility, but in such systems it may be easier to search for the second set of spectral lines (depending on the temperatures of the objects).

This effect should also be present in partially degenerate (sdB+WD) or non-degenerate binary systems. The precision on the eclipse times goes as  $\sqrt{\tau} \propto \sqrt{R_{\text{small}}}$ . If the binary is wide enough that the larger star(s) are undistorted by tides and hence the orbit remains strictly periodic, the overall detectability  $\Delta t_{\text{LT}}/\sigma_{t_e} \propto \sqrt{P/R_{\text{small}}}$  can actually increase over the double WD case I have been considering. Requiring  $a \propto R_{\text{large}}$  to minimize tidal distortions, which scale as  $(R_{\text{large}}/a)^3$ , for a system with a  $0.2 M_\odot$  M star one needs periods of  $\gtrsim 1$  day to have tidal effects that are as small as in the double WD systems. For the ingress/egress duration the radius of the smaller object  $R_{\text{small}}$  increases from  $\sim 0.01 R_\odot$  to  $\sim 0.1 R_\odot$  (for a  $0.1 M_\odot$  M star companion, for example), so if the period increases by more than a factor of 10 then the wide system is more easily detectable (the probability of eclipse does decrease as  $R/a$ , though, and both primary and secondary eclipses must be seen). However, the ephemeris must be known sufficiently well with tight enough limits on (or measurements of) eccentricity so that the light-travel delay is the only deviation from regularity (see below).

For NLTT 11748, I recognize that  $K_2$  is the radial velocity that was measured since the heavier object is the fainter one. So,  $q \approx 0.15/0.71 = 0.21$ ,  $K_2 = 271 \text{ km s}^{-1}$ , and  $P = 5.64 \text{ hr}$ , which give  $\Delta t_{\text{LT}} = 4.6 \text{ s}$ . Steinfadt et al. (2010b) measured individual eclipse times to  $\sim 10$  s, making it hard to detect an effect like this. However, this was using 45 s exposures on a 2 m telescope, while the ingress/egress duration was only  $\approx 20$  s. Increasing to 4 m or 8 m will improve the S/N of individual exposures by a factor of 4–16, and using a cadence better matched to the orbit will help

as well, driving eclipse time uncertainties to  $\lesssim 1$  s (as above). This is sufficient to detect  $\Delta t_{\text{LT}}$ ; below I discuss how well one can measure it and what constraints one can get from it.

## 2.2. Comparison With Eccentricity

The above discussion considered circular orbits. For eccentricity  $e > 0$  the situation changes. I note that the objects in Table 1 have orbits that are consistent with circular orbits, although quantitative limits for  $e$  are not always given. This follows from their expected evolutionary histories, where common-envelope evolution (Nelemans et al. 2000) should have circularized orbits. Nonetheless, in case our understanding of these systems is incorrect or some further evolution (such as interaction with another body) may have caused non-zero eccentricity, I consider the effect of a non-zero eccentricity on our detection of  $\Delta t_{\text{LT}}$ .

First, there are changes to the expression for  $\Delta t_{\text{LT}}$  (Fabrycky 2010):

$$\Delta t_{\text{LT}} = (\Delta t_{\text{LT}})_{e=0} \times \left( \frac{1-e^2}{1-e^2 \sin^2 \omega} \right) \approx (\Delta t_{\text{LT}})_{e=0} \times (1 - e^2 \cos^2 \omega + \dots) \quad (5)$$

where  $\omega$  is the argument of pericenter. As  $(\Delta t_{\text{LT}})_{e=0}$  is small to begin with, this is unlikely to be significant. More important, though, is that an additional term changes the relative timing of the primary and secondary eclipses. Following Winn (2010):

$$\Delta t_e \approx \frac{Pe}{\pi} \cos \omega \quad (6)$$

and the primary eclipse also changes duration relative to the secondary eclipse by the ratio  $1 + e \sin \omega$ . To compare  $\Delta t_{\text{LT}}$  and  $\Delta t_e$  means effectively comparing  $K_2(1-q)/c$  and  $e \cos \omega$ . For  $K_2 \sim 300 \text{ km s}^{-1}$ , this means that one is sensitive to  $e \sim 10^{-3}$  (although  $\omega$  is poorly determined for low  $e$ ). If it can be asserted for some independent reason (i.e., evolutionary assumptions) that  $e \ll 10^{-3}$  then one can treat any measured  $\Delta t$  as coming from light-travel delay. But if not one must be more careful.

Fortunately, eccentricity can be constrained from the radial velocities. Adopting the small- $e$  limit as in Lange et al. (2001),  $N_{\text{RV}}$  spectra can limit the eccentricity to  $\sigma_e \approx 2\sigma_v/K_2\sqrt{N_{\text{RV}}}$ , where  $\sigma_v$  is the precision of the individual velocity measurements (see also Gaudi & Winn 2007). With  $> 100$  observations with  $< 1 \text{ km s}^{-1}$  precision the eccentricity can be limited (independent of  $\omega$ ) to  $\ll 10^{-3}$ , and hence can identify whether any measured time delay has a contribution from an eccentric orbit. This requires dedicated radial velocity measurements over one or more full orbits, but is achievable with current instrumentation. At this level one must also account for additional effects such as light-travel delay in the spectroscopic analysis (Zucker & Alexander 2007). Tidal distortions can also mimic eccentricity in radial velocity fits (Eaton 2008), but these can be identified photometrically and are expected to be quite small,  $\sim 10^{-4}$ , except in the most compact systems.

## 2.3. Mass Constraints

Equation (4) gives an independent constraint on the mass ratio  $q$ , which helps break the degeneracy in the

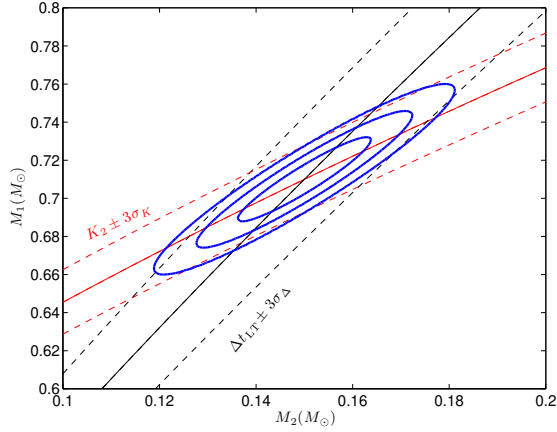


FIG. 1.— Constraints on individual masses from a single radial velocity constraint  $K_2$  and a light-travel delay  $\Delta t_{\text{LT}}$ . I show the constraints from each measurement individually (along with  $3\sigma$  ranges) as the diagonal lines. The contours show  $1\sigma$ ,  $2\sigma$ , and  $3\sigma$  joint confidence contours on  $M_1$  and  $M_2$ ; their covariance is apparent. This system has parameters similar to those of NLTT 11748, and I assumed  $\sigma_K = 1 \text{ km s}^{-1}$  and  $\sigma_\Delta = 50 \text{ ms}$ , which is rather optimistic.

mass function to measure the masses of the stars individually. For the individual masses

$$M_1 = \frac{K_2}{2\pi GP} (2PK_2 - \Delta t_{\text{LT}} \pi c)^2$$

$$M_2 = (2PK_2 - \Delta t_{\text{LT}} \pi c)^2 \left( \frac{K_2}{2\pi GP} - \frac{\Delta t_{\text{LT}} c}{2GP^2} \right). \quad (7)$$

Assume that I measure  $K_2 \pm \sigma_K$  and  $\Delta t_{\text{LT}} \pm \sigma_\Delta$  ( $P$  is typically known to much higher precision); I also assume  $e = 0$ . How well can I determine the individual masses? I know  $q$  to:

$$\sigma_q^2 = \frac{\pi^2 c^2}{P^2 K_2^4} (K_2^2 \sigma_\Delta^2 + \Delta t_{\text{LT}}^2 \sigma_K^2). \quad (8)$$

I now wish to see with what precision I can estimate the masses from the observations. Doing standard error propagation,

$$\frac{\partial M_1}{\partial K_2} = \left( \frac{PM^2}{2\pi G} \right)^{1/3} \frac{5+q}{(1+q)}$$

$$\left| \frac{\partial M_1}{\partial \Delta t_{\text{LT}}} \right| = \left( \frac{4\pi^2 M^2 c^3}{P^2 G} \right)^{1/3} \frac{1}{(1+q)}. \quad (9)$$

These are the contributions of the  $\sigma_K$  and  $\sigma_\Delta$  to the uncertainty on the mass, i.e.,  $\sigma_M^2 = \sigma_K^2 |\partial M / \partial K|^2 + \sigma_\Delta^2 |\partial M / \partial \Delta t_{\text{LT}}|^2$ . For the two terms to be comparable requires  $\sigma_\Delta = ((q+5)P/2\pi c)\sigma_K \approx 10P_{\text{hr}}\sigma_{K,\text{kms}} \text{ ms}$  (where  $P_{\text{hr}}$  is the period in hr and  $\sigma_{K,\text{kms}}$  is the uncertainty on  $K_2$  in  $\text{km s}^{-1}$ ). With those, I would have  $\sigma_{M_1} \sim 0.01M_\odot$  for periods  $P \gtrsim 1 \text{ hr}$  and mass ratios  $q \sim 0.25$ . The constraint on  $M_2$  is similar. I illustrate this in Figure 1, where I show mass constraints on NLTT 11748 from hypothetical time-delay measurements.

However, it is likely that the uncertainty from the radial velocity amplitude will be considerably less than that from  $\Delta t_{\text{LT}}$ : individual velocity measurements can easily have uncertainties of a few  $\text{km s}^{-1}$  with a large tele-

scope, and combining enough of them to give a meaningful constraint on the eccentricity will likewise end up with  $\sigma_K = \sigma_v / \sqrt{N_{\text{RV}}} < 1 \text{ km s}^{-1}$ . Getting a comparable constraint on the time delay seems implausible: with individual times measured to  $\sim 1 \text{ s}$ ,  $> 10^4$  eclipses are needed to get  $\sigma_\Delta < 10 \text{ ms}$ , and only one time delay is measurable per orbit. This means one needs significantly higher signal-to-noise per observation than the several hundred I have been assuming here or that I will be limited by  $\sigma_\Delta$ . In this case, the precision on  $M_1$  improves as  $\sigma_{M_1} \sim P^{-2/3}\sigma_\Delta$ ; including the difficulty in detecting the delay  $\sigma_\Delta \sim P^{1/6}$ , the determination of  $M_1$  improves as  $P^{-1/2}$ . The only ways that long periods are penalized are in terms of observing strategy, as for long periods the time to get enough eclipses measured will grow long as well, and for the probability of detecting an eclipse in the first place since that decreases as  $1/a$ .

As shown in Figure 1, the joint probability distribution for  $(M_1, M_2)$  is strongly correlated between  $M_1$  and  $M_2$ , with a much stronger constraint on  $M_2 - M_1$  than on  $M_2 + M_1$ . However, this would even be true—although to a lesser degree—if the other radial velocity amplitude  $K_1$  were measured, especially if it were at lower precision because it is much fainter. It is straightforward although tedious to compute the linear combinations of the masses that minimize/maximize the variance which would be preferred for fitting. While not perfect, with this constraint one would have a much better picture of the system.

### 3. CONCLUSIONS

Motivated by the recent discovery of NLTT 11748, the first eclipsing double WD binary, I have examined a phenomenon that affects precision eclipse timing of such a system. With knowledge of the individual masses, one can put much stronger constraints on the radii of the two WDs, the evolutionary history of the system, and its expected outcome, not to mention WD atmosphere models and models for the interiors of He WDs (e.g., Panei et al. 2007; Steinfadt et al. 2010a). This effect, a delay between perfect phasing of primary and secondary eclipses, can be used to constrain the individual masses of the binary, something difficult to do otherwise.

I find that the light-travel delay should be detectable in the case of NLTT 11748, and possibly in some other similar binary systems should they prove to have both primary and secondary eclipses: long periods are favored both for detecting  $\Delta t_{\text{LT}}$  and for using it to constrain the masses, although long periods do not favor detecting eclipses to begin with. The constraints on the individual masses can approach  $\pm 0.01M_\odot$  for plausible data-sets, and will likely be limited by the precision of the eclipse timing, suggesting that an intensive timing effort on large telescopes is worthwhile. Detection of a second radial velocity amplitude would over constrain the system, leading to even tighter determinations of the masses. In non-degenerate eclipsing binaries, such as those that *Kepler* may discover, the delay should also be detectable for systems with orbital periods of greater than a few days, although it requires that the mass ratio differs from one and that no other unmodeled orbit variations be present to a high degree of confidence.

The orbits of the binary members can also be per-

turbed by other bodies in the systems, either on shorter (planets or other small bodies in close orbits) or longer timescales (a distant body). In both cases, perturbations in transit timing may be visible (see Agol et al. 2005 for a detailed discussion). Given the wide variety in possible situations it is out of the scope of this Letter to consider, but any perceived variation in transit timing must be compared against the possible presence of additional bodies. There could also be effects that alter the perceived primary versus secondary eclipse times without altering the orbit, such as hot spots due to irradiation (Knutson et al. 2007; Agol et al. 2010) or accretion. For the former, I note that the incoming radiation in the double WD systems is typically very small,  $\sim 10^{-3}$  of the outgoing radiation. As for accretion, both WDs are well inside their Roche lobes and so none is expected.

I find the fortunate coincidence that NLTT 11748, the one object known to be eclipsing, also has the binary parameters that lead to the highest value of  $\Delta t_{LT}$  among similar double WD binaries. Hopefully, with dedicated observing this effect will be detected and can constrain the NLTT 11748 system even more than is possible today.

I thank the anonymous referee, as well as L. Bildsten, T. Marsh, J. Winn, E. Agol, D. Fabrycky, S. Gaudi, M. van Adelsberg, and R. Cooper for helpful discussions. DLK was supported by NASA through Hubble Fellowship Grant #01207.01-A awarded by the STScI which is operated by AURA, Inc., for NASA, under contract NAS 5-26555. This work was supported by the NSF under grants PHY 05-51164 and AST 07-07633.

## REFERENCES

- Agol, E., Cowan, N. B., Knutson, H., Deming, D. L., Steffen, J. H., Henry, G. W., & Charbonneau, D. 2010, *ApJ*, submitted
- Agol, E., Steffen, J., Sari, R., & Clarkson, W. 2005, *MNRAS*, 359, 567
- Althaus, L. G. & Benvenuto, O. G. 1998, *MNRAS*, 296, 206
- Badenes, C., Mullally, F., Thompson, S. E., & Lupton, R. H. 2009, *ApJ*, 707, 971
- Blandford, R. & Teukolsky, S. A. 1976, *ApJ*, 205, 580
- Brown, T. M., Charbonneau, D., Gilliland, R. L., Noyes, R. W., & Burrows, A. 2001, *ApJ*, 552, 699
- Carter, J. A. & Winn, J. N. 2009, *ApJ*, 704, 51
- Carter, J. A., Yee, J. C., Eastman, J., Gaudi, B. S., & Winn, J. N. 2008, *ApJ*, 689, 499
- Charbonneau, D., Brown, T. M., Latham, D. W., & Mayor, M. 2000, *ApJ*, 529, L45
- Deeg, H. J., Doyle, L. R., Kozhevnikov, V. P., Blue, J. E., Martín, E. L., & Schneider, J. 2000, *A&A*, 358, L5
- Doyle, L. R., et al. 1998, in *ASP Conf. Ser. 134, Brown Dwarfs and Extrasolar Planets*, ed. R. Rebolo, E. L. Martín, & M. R. Zapatero Osorio, (San Francisco, CA: ASP) 224
- Eaton, J. A. 2008, *ApJ*, 681, 562
- Fabrycky, D. C. 2010, *Non-Keplerian Dynamics*, in *Extra-Solar Planets*, ed. S. Seager (Tucson, AZ: Univ. Arizona)
- Gaudi, B. S. & Winn, J. N. 2007, *ApJ*, 655, 550
- Hebrard, G., et al. 2010, *A&A*, in press, arXiv:1004.0790
- Holman, M. J. & Murray, N. W. 2005, *Science*, 307, 1288
- Hulse, R. A. & Taylor, J. H. 1975, *ApJ*, 195, L51
- Iben, I., Jr., & Tutukov, A. V. 1984, *ApJS*, 54, 335
- Kawka, A. & Vennes, S. 2009, *A&A*, 506, L25
- Kilic, M., Brown, W. R., Allende Prieto, C., & Kenyon, S. J. 2010, *ApJ*, 716, 122
- Knutson, H. A., Charbonneau, D., Noyes, R. W., Brown, T. M., & Gilliland, R. L. 2007, *ApJ*, 655, 564
- Kulkarni, S. R. & van Kerkwijk, M. H. 2010, *ApJ*, in press, arXiv:1003.2169
- Lange, C., Camilo, F., Wex, N., Kramer, M., Backer, D. C., Lyne, A. G., & Doroshenko, O. 2001, *MNRAS*, 326, 274
- Lee, J. W., Kim, S., Kim, C., Koch, R. H., Lee, C., Kim, H., & Park, J. 2009, *AJ*, 137, 3181
- Liebert, J., Bergeron, P., & Holberg, J. B. 2005, *ApJS*, 156, 47
- Loeb, A. 2005, *ApJ*, 623, L45
- Lorimer, D. R. & Kramer, M. 2004, *Handbook of Pulsar Astronomy* (Cambridge: Cambridge Univ. Press)
- Marsh, T. R., Dhillon, V. S., & Duck, S. R. 1995, *MNRAS*, 275, 828
- Marsh, T. R., Gaensicke, B. T., Steeghs, D., Southworth, J., Koester, D., Harris, V., & Merry, L. 2010, *ApJ*, in press, arXiv:1002.4677
- Miralda-Escudé, J. 2002, *ApJ*, 564, 1019
- Mullally, F., Badenes, C., Thompson, S. E., & Lupton, R. 2009, *ApJ*, 707, L51
- Nelemans, G. 2009, *Class. Quantum Grav.*, 26, 094030
- Nelemans, G., et al. 2005, *A&A*, 440, 1087
- Nelemans, G., Verbunt, F., Yungelson, L. R., & Portegies Zwart, S. F. 2000, *A&A*, 360, 1011
- Nelemans, G., Yungelson, L. R., Portegies Zwart, S. F., & Verbunt, F. 2001, *A&A*, 365, 491
- Panei, J. A., Althaus, L. G., Chen, X., & Han, Z. 2007, *MNRAS*, 382, 779
- Qian, S., Dai, Z., Liao, W., Zhu, L., Liu, L., & Zhao, E. G. 2009, *ApJ*, 706, L96
- Rafikov, R. R. 2009, *ApJ*, 700, 965
- Schneider, J. & Doyle, L. R. 1995, *Earth Moon Planets*, 71, 153
- Steinfadt, J. D. R., Bildsten, L., & Arras, P. 2010a, *ApJ*, in press, arXiv:1005.5423
- Steinfadt, J. D. R., Kaplan, D. L., Shporer, A., Bildsten, L., & Howell, S. B. 2010b, *ApJ*, 716, L146
- Sterken, C. (ed.) 2005a, *ASP Conf. Ser. 335, The Light-Time Effect in Astrophysics: Causes and Cures of the O-C Diagram* (San Francisco, CA: ASP)
- Sterken, C. 2005b, in *ASP Conf. Ser. 335, The Light-Time Effect in Astrophysics: Causes and Cures of the O-C Diagram*, ed. C. Sterken (San Francisco, CA: ASP), 181
- Sybilski, P., Konacki, M., & Kozłowski, S. 2010, *MNRAS*, 414
- Thorsett, S. E. & Chakrabarty, D. 1999, *ApJ*, 512, 288
- Webbink, R. F. 1984, *ApJ*, 277, 355
- Winn, J. N. 2010, *Transits and Occultations*, in *Extra-Solar Planets*, ed. S. Seager (Tucson, AZ: Univ. Arizona), arXiv:1001.2010
- Zucker, S. & Alexander, T. 2007, *ApJ*, 654, L83